DOI 10.1007/s11055-021-01059-5
Neuroscience and Behavioral Physiology, Vol. 51, No. 2, February, 2021

Long-Term Sequelae of Traumatic Brain Injury in Rats: A Morphological, Behavioral, and Electrophysiological Study

I. G. Komoltsev,[1,2] A. A. Volkova,[1,3] I. P. Levshina,[1*] M. R. Novikova,[1] and N. V. Gulyaeva[1,2]

UDC 612.821.6

Translated from Zhurnal Vysshei Nervnoi Deyatel'nosti imeni I. P. Pavlova, Vol. 70, No. 4, pp. 500–514, July–August, 2020. Original article submitted September 6, 2019. Revised version received December 2, 2019. Accepted December 16, 2019.

The long-term sequelae of traumatic brain injury (TBI) in humans are linked with the development of convulsions and cognitive and emotional disorders and are also associated with acceleration of brain aging processes and the formation of hippocampal sclerosis (HS). The mechanisms of these complications remain incompletely understood and treatment is extremely difficult. Existing data obtained using experimental models in animals do not provide a clear assessment of these mechanisms. The present study clarifies the long-term histological, behavioral, and electrophysiological sequelae of TBI in rats. Six months after lateral hydrodynamic blows, animals displayed severe asymmetrical gliosis in hippocampal field CA3 and the dental gyrus in the form of fibrillary astrogliosis, with an increase in the number of glial cells and depletion of the pyramidal layer of field CA3 in the ipsilateral hemisphere (corresponding to type 3 HS in humans); sham-operated animals displayed only symmetrical gliosis (isolated gliosis in the human HS classification). The behavior of the rats six months after TBI and the sham procedure was characterized by decreases in motor activity, which some signs of increased anxiety. Behavioral impairments were more severe in rats after TBI, mainly due to decreases in exploratory activity. The long-term period of TBI was characterized on ECoG by prolonged spike-wave discharges in the cortex and asymmetry of epileptiform spikes in the hippocampus. Two rats in the late period demonstrated epileptic seizures. Intense brain aging processes in rats with TBI and the development of neurodegenerative changes in the hippocampus may be linked with chronic remote neuroinflammation, which plays an important role in the development of posttraumatic epilepsy and dementia.

Keywords: traumatic brain injury, hippocampal sclerosis, neurodegeneration, neuroinflammation, behavior, epileptogenesis.

Introduction. Traumatic brain injury is a serious risk factor for neurological and psychiatric disorders in the long-term period of trauma: more than half of patients develop emotional and cognitive disorders and sleep impairments, while 10–20% develop posttraumatic epilepsy (PTE) [Jorge and David, 2012; Christensen, 2015]. The presence of TBI in the history is in important risk factor for dementia in elderly people [Wood, 2017; Fann et al., 2018]. Degenerative changes on MRI scans in patients with TBI are apparent at earlier age than in control subjects without TBI [Cole et al., 2015]. This points to faster "brain aging" (atrophy in various areas) in patients with histories of trauma, whose severity correlates with cognitive impairments. The mechanisms of these changes remain incompletely understood. The process of acute damage due to TBI are characterized by damage to the BBB, attraction of immune cells, activation of the resident microglia, reactive astrogliosis, and production of pro- and anti-inflammatory cytokines in response to the appearance of damage-associated molecular frag-

[1] Laboratory for Functional Biochemistry of the Nervous System, Institute of Higher Nervous Activity and Neurophysiology, Russian Academy of Sciences, Moscow, Russia; e-mail: komoltsev.ilia@gmail.com.
[2] Solov'ev Scientific-Applied Psychoneurology Center, Moscow Health Department, Moscow, Russia.
[3] Pirogov Russian National Research Medical University, Russian Ministry of Health, Moscow, Russia.
[*] Deceased.

ments which trigger inflammatory processes [Thompson et al., 2005; Simon et al., 2017]. In the long-term period of TBI (more than a week after trauma), acute neuroinflammation progresses to the chronic phase. Activation of the microglia and production of proinflammatory mediators are accompanied by further death of neurons and progressive atrophy [Puntambekar et al., 2018]. The development of remote chronic neuroinflammatory processes in the hippocampus can lead to the formation of cognitive deficit and emotional impairments in the late period of TBI [Vezzani et al., 2012]. Chronic neuroinflammation is accompanied by parallel processes of neurogenesis and neuroplasticity, which are entrained to restore brain functions lost as a result of neuron death, though in some cases they promote the development of aberrant neural networks producing late epileptic seizures [Gulyaeva, 2010]. Despite active studies, the mechanisms and early predictors of the development of PTE remain to be identified. In our previous study, we demonstrated both the presence of epileptiform activity in the cortex and hippocampus and remote hippocampal damage (arising at a distance from the focus in the cortex) in the absence of epileptic discharges in the acute period of TBI in rats [Komoltsev et al., 2018]. In addition, in the acute period of TBI, we identified elements of anxiety behavior associated with decreases in the proportion of REM sleep [Komoltsev et al., 2017]. The aim of the present work was to carry out a complex characterization of changes in the late period of TBI in rats in comparison with results obtained in previous studies. The experimental tasks were to assess morphological changes in the hippocampus and the relationship between the histological picture and the current classification of hippocampal sclerosis in humans, to characterize behavioral changes in the late period of TBI, and to identify epileptic seizures and epileptiform activity in animals at six months after trauma.

Methods. Animal experiments were performed in compliance with the requirements of Directive 2010/63/EU of the European Parliament and Council of September 22, 2010, an Order No. 267 of the Ministry of Health of the Russian Federation of June 19, 2003, regarding the protection and use of animals in experimental research. The experimental protocol was approved by the Ethics Committee of the Institute of Higher Nervous Activity and Neurophysiology, Russian Academy of Sciences (protocol No. 10 of December 10, 2012). All measures for reducing the number of animals used and minimizing their suffering were taken. Experiments were performed on 20 male Wistar rats from the Pushchino animal laboratory aged about six months (weight 400–500 g) when the experiments started; rats were divided into two groups – rats with TBI (n = 13, three excluded) and sham-operated rats (SO, n = 7, one excluded). Animals with damage to the integrity of the dura mater were excluded (1 TBI, 1 SO). Mortality at six months was 16% (two rats of the TBI group). All further calculations were based on 10 rats of the TBI group and six of the SO group. During the experiment, rats lost no more than 10% of body weight.

Surgical preparation and modeling of TBI. TBI was applied using a lateral hydrodynamic blow model [McIntosh et al., 1989; Kabadi et al., 2010]. Operations were performed under 1–3% isoflurane anesthesia. After scalping, all animals underwent trepanning of the skull (AP = 3, L = 3, projection of the right sensorimotor cortex, opening diameter 3 mm). We have previously described the immediate area of damage in this TBI application protocol [Komoltsev, et al., 2019], which includes the sensory (representation of the abdomen and whiskers), parietal, auditory, and visual areas of the neocortex. The head of a Luer-type injection needle was established at the edges of the trepanned opening. After complete recovery of rats from anesthesia, the head of the needle was connected via rigid plastic tube to a Fluid Percussion Device with PC-Based Measurement Unit model FP302, USA. Rats of the TBI group, in conditions of free behavior, received a blow of force 2.4–3.6 atmospheres. The needle head was removed from all animals and openings were covered with a bone patch and the edges of the wound were fixed.

Behavioral testing. Testing of initial behavioral activity was performed one month before craniotomy (at age five months). Motor and exploratory activity and elements of anxiety behavior were evaluated in the open field (OF) test, the elevated plus maze (EPM) test, and the Porsolt test over three days in this order. Repeat testing in the OF and EPM were run three and two days, respectively, before electrode implantation, at age 12 months (six months after TBI). The repeat Porsolt test was performed after a seven-day EEG recording period before animals were removed from the experiments.

The EPM assesses animals' anxiety levels [Bailey and Crawley, 2009]. Maze arms were 50 cm long and the floor was divided into segments of 10 cm for assessment of paths covered. Arms were 10 cm wide, the central platform was of size 10 × 10 cm, and the walls of the closed arms were 10 cm high. Illumination was 6–8 lx in the closed arms and 12–15 lx in the open arms. The rat was placed on the central platform of the EPM facing an open arm. The duration of the first stay by the rat in the central platform (the latent period, LP), the time taken to choose an arm on crossing the central platform (i.e., the total time spent on the central platform without considering the LP), and the number of crossings were determined. Numbers of squares crossed were measured and were used to calculate the path covered in the maze arms. Rats' exploratory activity was evaluated in terms of the total number of rearings and hangings, and the numbers of peeps out of and peeps into the arms were counted. The arms and central area were regarded as departed when all four paws were outside the corresponding square. The times spent in the open and closed arms of the maze were determined, along with the numbers of entries into the open and closed arms. The total time spent in the maze was 300 sec.

The OF test evaluates activity and anxiety. The experiment used a round open field with a diameter of 100 cm, the floor being divided into squares of size 10 × 10 cm for assessment of paths covered. Wall height was 30 cm. The times spent in the central and peripheral parts of the OF were measured, along with the number of crossings of the center of the OF. Horizontal activity was assessed in terms of path covered and vertical activity was measured in terms of rearings; autonomic reactions were assessed from defecations and urinations. The total duration of the test was 300 sec. Experiments were analyzed using video recordings in the Noldus automatic processing program. The forced swimming test (Porsolt test) was performed in a tall, transparent cylindrical glass (height 65 cm, diameter 30 cm) filled to a depth of 55 cm with warm (23–24°C) water. The rat was placed in the center of the glass and its behavior was recorded using a video camera. The total duration of the test was 300 sec. Video recordings were used to determine the total durations of active and passive swimming (immobility) and the numbers of freezing episodes and dives and their durations.

EEG recording and processing. Six months after the first surgery and one day after completion of repeat behavioral tests, rats were scalped and five animals ($n = 3$ for TBI and $n = 2$ for SO)) underwent implantation of electrodes (under anesthesia with 1–3% isoflurane) into the frontal and occipital areas of the cortex and the dentate fascia of the dorsal and ventral hippocampus (coordinates are given in mm: on the rostrocaudal axis from the bregma, laterally from the midline, depth from the bone surface): left rostral (LR: 1, –3); right rostral (RR: 1, 3); left caudal (LC: –7, –3); right caudal (RC: –7, 3); left ventral hippocampus (LVH: –6, –4, 4.3); left dorsal hippocampus (LDH: 0, –2, 5.3); right ventral hippocampus (RVH: –6, 4, 4.3); right dorsal hippocampus (RDH: 0, 2, 5.3). The reference electrode was implanted over the cerebellum along the midline and the ground electrode was positioned rostral to the olfactory bulbs on the left of the midline. EEG and video recordings were made in separate chambers with free access to water and food and natural illumination for seven experimental days after the behavioral tests. BR8V1 (BioRecorder) wireless eight-channel biopotentials amplifiers were used, with 24-bit ADC, input range up to 1200 mV, digitization frequency 1 kHz, sampling frequency 250 Hz. Traces were assessed in the program EDF browser 1.57 using a Butterworth filter with a lower limit of 1 Hz and an upper limit of 30 Hz, divided into 20-sec epochs. Analysis of sleep structure was based on 15 sleep–waking cycles for each rat: phases of the sleep–waking cycle were identified for each epoch: NREM sleep (slow-wave sleep phase), REM sleep (rapid sleep phase), or waking phase. The amplitude of epileptiform activity in the hippocampus was compared by computing the ratio of spike amplitude in the left and right hippocampus and comparing the resulting ratio for each spike with the mean ratio obtained for all spikes. This approach decreases variation in the amplitude of activity associated with a specific animal by comparing the ratio of amplitudes. The ratio for the dorsal hippocampus was 1.5, compared with 1.1 for the ventral hippocampus. The durations of spike-slow wave complexes in the cortex were also measured.

Morphological analysis. At six months after TBI and one week after recording the EEG, rats were anesthetized with chloral hydrate (450 mg/kg) and harvested from experiments by intracardiac perfusion with 4% paraformaldehyde solution in 0.1 M phosphate buffer pH 7.4 using a Heidolph Pumpdrive 5001 pump. Vibratome frontal slices of thickness 50 μm were cut on a Campden Instruments MA6752 Vibroslice microtome. Slices from the area 2.8 mm to 5.6 mm caudal to the bregma were analyzed (distance between slices at least 600 μm) after staining with cresyl violet by the Nissl method. Immunocytochemical staining was for the microglial marker GFAP (diluted 1:500, Dako, Denmark). Morphometry in ImageJ used images magnified ×20 (Keyence BZ-X700 Fluorescence Microscope). Quantitative analysis was performed using four slices stained for GFAP and four slices stained by the Nissl method from each animal. All counts were carried out on both the ipsilateral and contralateral hemispheres. Slices stained by the Nissl method were used to measure the thickness of the granular layer of the dentate gyrus (DG) and the pyramidal layer of fields CA1 and CA3 of both hemispheres. Three measurements were made for each field on each slice and values were averaged. The same slices were used for counting the numbers of glial cells throughout the polymorphic layer of the dentate gyrus and the radial layer (radial dendritic layer) of fields CA1 and CA3. Nerve cells on slices were identified from the presence of stained neuron bodies and Nissl substance in the cytoplasm, glial cells being discriminated on the basis of nuclear staining intensity and the absence of stained cytoplasm. Astrocyte numbers were counted in slices stained for GFAP (a specific marker for astrocytes) using three fields of view of 150 × 150 μm in each area (DG, CA1, CA3) on each slice. Values from the three measurements in each area were averaged. The extent of hippocampal gliosis was determined using a points scheme (0–3 points) on slices stained for GFAP.

Statistical methods. Calculations were run in Statistica 12 (StatSoft Inc.). The TBI and SO groups were compared using the Mann–Whitney test; within-group time points were compared using the Wilcoxon test. Ratios of discharge duration and spike asymmetries were measured in the electrophysiological part of the study using the two-way Fisher's exact test. Results are presented as mean ± standard error of the mean.

Results. ***Morphological changes in the hippocampus in rats six months after TBI.*** Morphological changes in rats in the long-term period of TBI and sham-operated animals were compared with the classification of human hippocampal sclerosis (HS). HS in histological studies in humans and experimental studies was confirmed (1) by the presence of

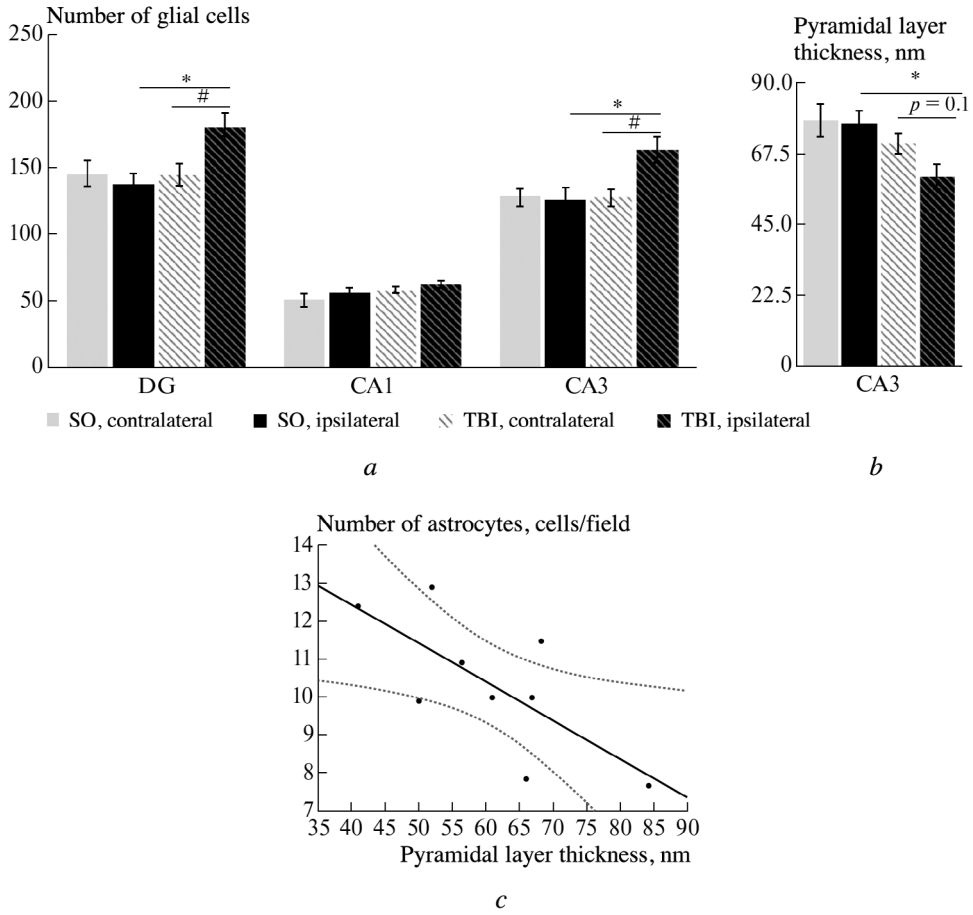

Fig. 1. Gliosis and thinning of neuron layers in the hippocampus six months after TBI. *a*) Number of glial cells in the rat hippocampus after TBI, stained by the Nissl method. *b*) Thickness of the pyramidal neuron layer in the rat hippocampus after TBI. *c*) Correlation between thinning of the pyramidal layer in field CA3 and the number of astroglial cells in rats after TBI (stained for GFAP) – the pyramidal layer was thinner in rats with severe gliosis ($p < 0.05$). *Comparison of TBI and SO groups $p < 0.05$, Mann–Whitney test. #Comparison of hemispheres in rats of the TBI group, $p < 0.05$, Wilcoxon test (dependent variables).

astrocyte gliosis and (2) depletion of the cellular layers in the hippocampus (due to neuron death).

Hippocampal gliosis. Nissl staining in rats with TBI showed increases in the numbers of glial cells (without differentiation into astrocytes, microglia, and other non-neuronal cells) in areas DG and CA3 in the ipsilateral hemisphere as compared with the contralateral, and also in the ipsilateral hippocampus of rats with TBI as compared with rats of the SO group (Fig. 1, *a*).

Astrocyte gliosis in the hippocampus. Astrocyte gliosis includes an increase in the number of cells and alterations in their morphology – increases in the number and length of processes and enlargement of astrocyte bodies. Analysis of slices demonstrated moderate astrocyte gliosis in the hippocampus in rats of both groups (SO and TBI), more clearly apparent in field CA3 and the dentate gyrus of the hippocampus (Fig. 2, *a*). Five rats (one SO and four TBI) showed significant fibrillary astrogliosis in the DG (three points); gliosis of 2 and 3 points was seen in 10 rats (two SO and eight TBI). Astrocytes themselves had morphology typical of the activated state – large, ameboid in shape, few processes, and sometimes with perifocal edema. Our previous studies showed that these changes in the astrocyte glia were not seen in young animals [Komoltsev et al., 2018]. No significant differences in astrocyte density in the hippocampal fields were seen between the SO and TBI groups, though changes in the hippocampus in the TBI group were markedly asymmetrical (Fig. 2, *b*). No differences between hemispheres were seen in the SO group. Astrocytes in the ipsilateral hippocampus of rats with TBI displayed less marked activatory morphology: the moderate level of gliosis in the ipsilateral hemisphere was greater than that in the contralateral hemisphere (1 ± 0.2 points in the contralateral and 2.1 ± 0.3 in the ipsilateral), $p < 0.05$; Fig. 2, *b*); the number of astrocytes per slice in field CA3 in rats of the TBI group was greater in the ipsilateral hemisphere (10.5 ± 0.6 cells vs. 8.9 ± 0.4 cells, $p < 0.05$). No interhemisphere differences were seen in the SO group (8.9 ± 0.5 and 8.7 ± 0.7 in the ipsilateral and contralateral hemispheres, respectively, $p > 0.1$). Thus, astrocyte hypertrophy occurred in all ani-

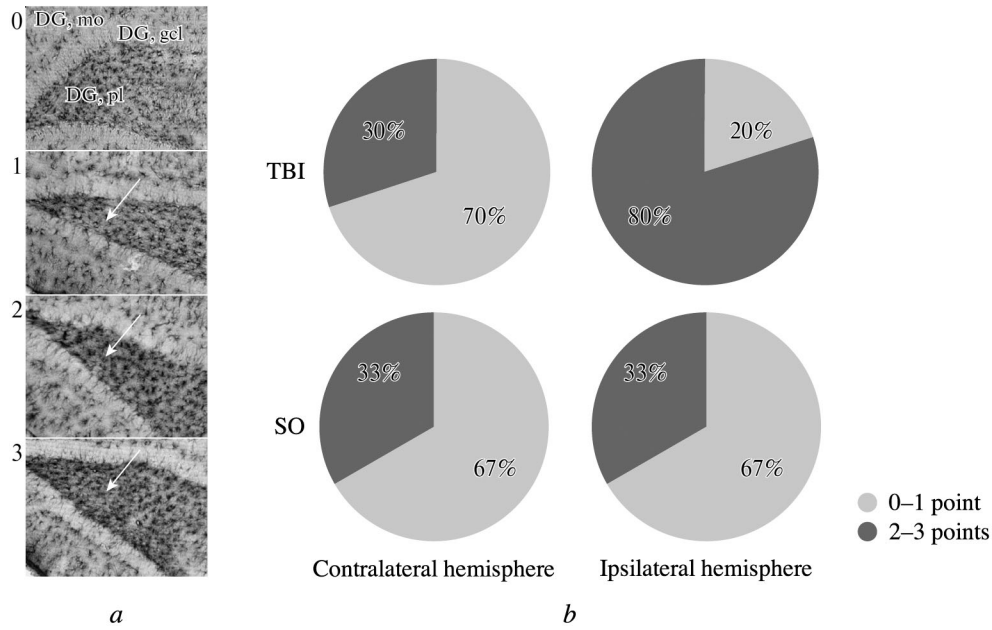

Fig. 2. Astrocyte gliosis in the hippocampus in rats six months after TBI. *a*) Scale of astrocyte gliosis in the dentate gurus of the hippocampus (0–3 points, changes shown by arrows); 3 points corresponds to fibrillar astrocyte gliosis. *b*) Glial scarring of different extents in rats of the SO and TBI groups in the ipsilateral and contralateral hemispheres. Asymmetry in astrocyte gliosis was noted in rats of the TBI group (in 80% of rats, the ipsilateral hemisphere showed gliosis rated at 2–3 points). DG, mo – molecular layer of the dentate gyrus, DG gcl – granular cell layer, DG pl – polymorphic layer of the dentate gyrus.

mals regardless of TBI and was probably linked with age. Changes in rats with TBI showed pronounced asymmetry the number of field CA3 astrocytes and the level of astrocyte gliosis were greater in the ipsilateral hippocampus.

Thinning and dispersion of the neuronal layers in the hippocampus. Thinning of the pyramidal layer in field CA3 of the ipsilateral hippocampus was seen in rats of the TBI group as compared with animals of the SO group (Fig. 1, *b*). No such differences were seen in the contralateral hemisphere. Differences between the ipsilateral and contralateral hemispheres in rats of the TBI group were seen at the level of a statistical trend ($p = 0.1$). Thinning of the pyramidal layer of field CA3 in the ipsilateral hippocampus in rats with TBI correlated with the number of astrocytes in this area ($r = 0.51, p = 0.03$; Fig. 1, *c*), which was not seen in the SO group ($r = 0.47, p = 0.35$). There were no differences in the thickness of the neuron layer in field CA1 and the DG in both hemispheres in TBI and SO rats. Thus, the age-related changes in astrocytes described above in rats with TBI displayed interhemisphere asymmetry and were accompanied by thinning of the pyramidal layer of CA3 in the ipsilateral hemisphere. In addition, 11 rats (four SO and seven TBI) showed dispersion of the pyramidal layer in hippocampal field CA3 (impairment of the compact structure of the cellular layer typical of patients with temporal epilepsy [Houser et al., 1990]).

Thus, the astrocyte gliosis in the hippocampus in rats following TBI detected on staining for GFAP was not qualitatively distinct from astrocyte gliosis associated with the animals' age. In the long-term period, TBI produced thinning of the pyramidal layer in field CA3, pronounced asymmetry of astrocyte gliosis in the ipsilateral hippocampus, and increases in the number of glial cells. The pattern of astrocyte gliosis and thinning of the hippocampal layers allowed HS in rats of the SO group to be classified as isolated gliosis and that in rats with TBI as type 3 HS [Blümcke et al., 2013], though the changes were also less pronounced and were seen mainly on quantitative pathomorphological analysis in rats of the TBI and SO groups as above.

Behavioral changes six months after TBI. Morphological changes in humans associated with age and/or TBI correlate with cognitive impairments [Cole et al., 2015]. The behavioral part of our study assessed age-related changes in the behavior of all rats (as compared with values before trauma and six months after TBI) and detected those changes which were more pronounced in rats with TBI (on comparison of the TBI and SO groups at six months post-trauma).

Behavioral changes in the long-term period of TBI. In the EPM at six months after trauma, rats of the TBI group, as compared with those of the SO group, showed smaller numbers of peeps out of and peeps into the maze arms (3.6 ± 0.7 in the TBI group vs. 6.3 ± 0.3 in the SO group, $p < 0.05$); initial values in the TBI and SO groups were not significantly different ($4.6 \pm 0{,}6$ and 6.5 ± 1, respectively, $p > 0.1$). Comparison with initial levels (before surgery, at age five months) showed that rats after trauma displayed a significant reduction in the time spent in the central area

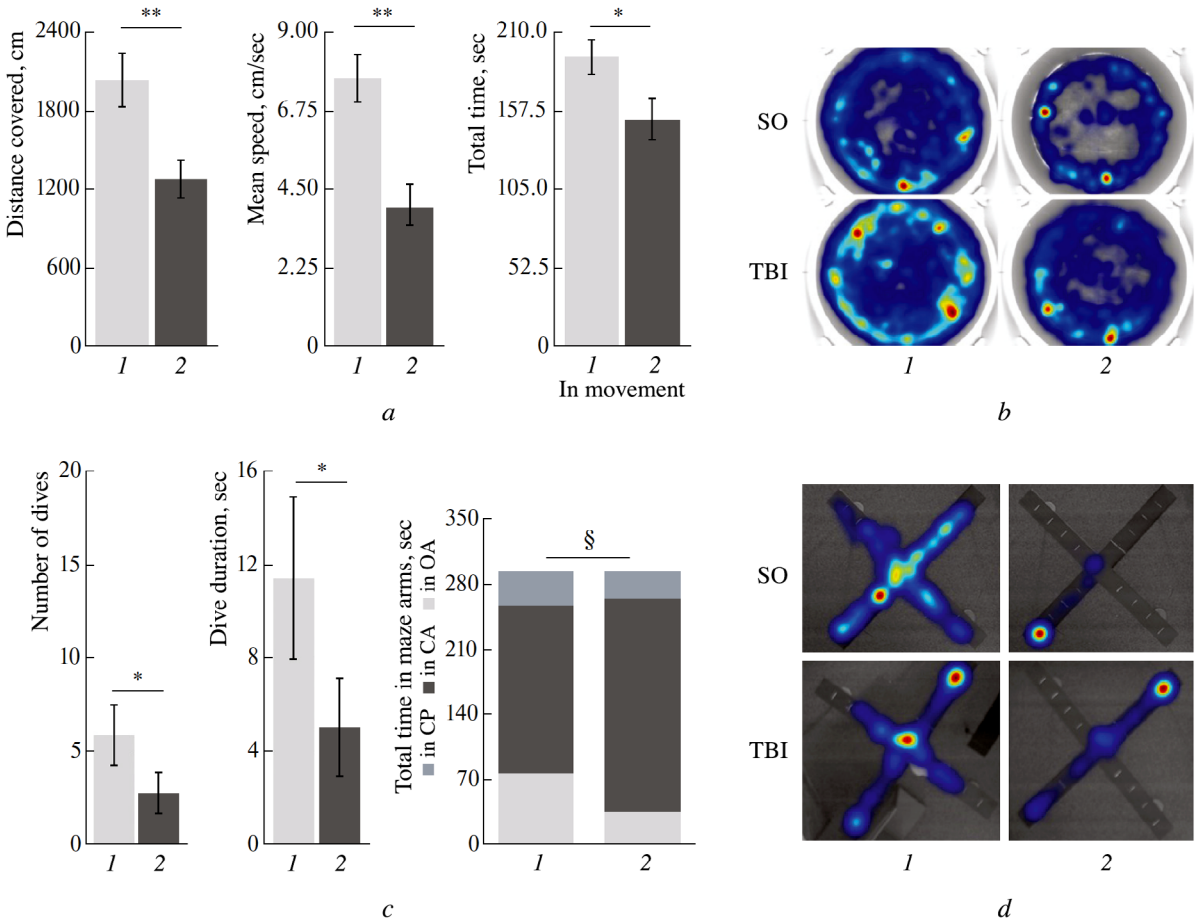

Fig. 3. Age-related behavioral changes in the open field (OF), elevated plus maze (EPM), and Porsolt tests. *a*) Behavior in the OF on initial testing and six months after craniotomy. *b*) Heat maps of behavior in the OF of rats of the SO and TBI groups on initial testing and six months after craniotomy. *c*) Behavior in the Porsolt test in rats in the initial state and six months after craniotomy. *d*) Behavior in the EPM on initial testing and six months after craniotomy. *e*) Heat maps of behavior in the EPM of rats of the TBI and SO groups at baseline and six months after craniotomy. *1*) Baseline; *2*) 6 months. Comparison with initial testing and six months after craniotomy, $^{*}p < 0.05$, $^{**}p < 0.01$, Wilcoxon test (dependent variables). Comparison of time in the CA and the OA on initial testing and six months after craniotomy, $^{\S}p < 0.05$, Wilcoxon test (dependent variables).

(from 44.4 ± 19.9 sec to 0 sec, $p < 0.05$) – after departure from the central platform (CP) into an arm of the maze, the rat did not exit to the center. Furthermore, these animals showed decreased exploratory activity – the sum of the numbers of rearings and hangings decreased six months after TBI (from 13.6 ± 1.2 to 8.6 ± 1.4, $p < 0.05$). These differences between the data obtained at ages five and 12 months were not seen in rats of the SO group; the initial total number of hangings and rearings was 12.0 ± 0.9, while the number six months after sham operations was 10.5 ± 1.8 ($p > 0.1$); the time spent in the central area by rats of the SO group decreased but not significantly – the initial time in the CP was 52 ± 21 sec, while six months after sham surgery it was 15 ± 15 sec ($p > 0.1$). The OF and Porsolt test showed no differences between the SO and TBI groups.

Age-related changes in the behavior of rats. At age one year, all animals became less active then they had been at age five months. The EPM (Fig. 3, *d*, *e*) showed decreases in the time spent in the open arms (OA) with simultaneous increases in the time spent in the closed arms (CA). There were no changes in the numbers of center crossings and entries into the closed arms in all rats (TBI and SO) on comparison of the test results at ages five and 12 months, while the number of entries into the open arms decreased (7 ± 1 on first testing vs. 4 ± 1 at six months after TBI, $p < 0.05$). The distance covered in the EPM test showed no change. The distance covered and the mean speed of travel in the OF test decreased (Fig. 3, *a*, *b*). The time spent by animals in movement decreased and the time spent immobile increased. The number of excursions to the center of the OF and the time spent in the center did not change in rats. In the Porsolt test (Fig. 3, *c*), all animals six months after surgery showed significant reductions in the number of dives and their duration. The durations of active swimming and immobility did not change.

Thus, six months after TBI and sham surgery, all animals showed marked reductions in movement activity, and some behavioral changes on this background could be explained

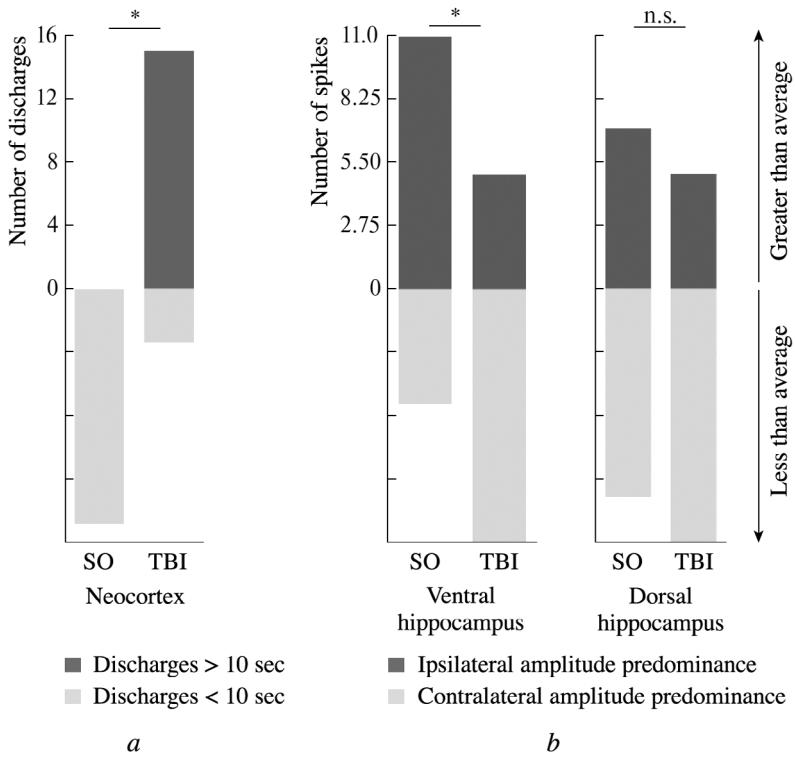

Fig. 4. Electrophysiological changes six months after TBI. *a*) The number of discharges greater than the mean (10 sec) was greater in rats of the TBI group. *b*) The number of spikes with amplitude dominance is greater in the contralateral hippocampus in rats of the TBI group, indicating asymmetry of high-amplitude activity in the hippocampus. *Fisher's exact test, $p < 0.05$.

by increased anxiety (increased time spent in the closed arms of the EPM with no change in the number of crossings of the center). Rats with TBI showed a reduction in exploratory activity on comparison with rats of the SO group.

Electrophysiological changes six months after TBI. The long-term period of TBI in some animals could be accompanied by the appearance of epileptic seizures and epileptiform activity. We analyzed epileptiform activity in the cortex and hippocampus. The presence of epileptic seizures was confirmed by video analysis.

Epileptiform activity six months after TBI. Implantation of electrodes six months after TBI involved repeat scalping of the rats. Animals with changes in the skull bones as a result of the first operation found during repeat scalping did not undergo electrode implantation because of the impossibility of accurately identifying electrode implantation sites and reliable fixation with dental cement. Recording of the ECoG and field potentials was performed in five rats (three TBI and two SO).

At six months after TBI, the cortical EEG showed discharges in the form of spike-slow wave complexes at a frequency of about 7 Hz. These discharges have been described not only in rats in models of genetic and acquired epilepsy, but also in control animals [Rodgers et al., 2015]. Mean discharge duration in rats six months after surgery was 9.7 ± 1.5 sec, though the number of discharges with durations greater than the mean was significantly greater in animals with TBI ($p < 0.05$) (Fig. 4, *a*). In the SO group, discharge duration was 2.6 ± 1.4 sec, which was no different from discharge duration in 18-month-old rats in our previous studies [Komoltsev et al., 2018].

Electrographic epileptic seizures were recorded in two of the three TBI rats with implanted electrodes (Fig. 5). In one rat with a large number of prolonged (>10 sec) cortical discharges, the occurrence of activity corresponding to freezing of the animal on the accelerometer, which was confirmed on the video recording. This may correspond to the nonmotor epileptic seizures described in models of posttraumatic epilepsy. Another rat six months after TBI displayed myoclonic seizures accompanied by spike-wave activity in the cortex, which differed in frequency from the previous (about 1.5 Hz). Each discharge was accompanied by twitching of the rat, as assessed on the video recording and accelerometer.

Electrical activity in the hippocampus. Six months after TBI, rats showed pronounced asymmetry in spike amplitude in the ventral but not the dorsal hippocampus (Fig. 4, *b*). These data confirm that rats with trauma had functional changes accompanied by morphological asymmetry as described above.

The sleep-waking cycle in rats six months after TBI. Our previous studies identified impairments to the ratio of the phases of the sleep–waking cycle in the acute period of TBI. The present study did not reveal any changes in the

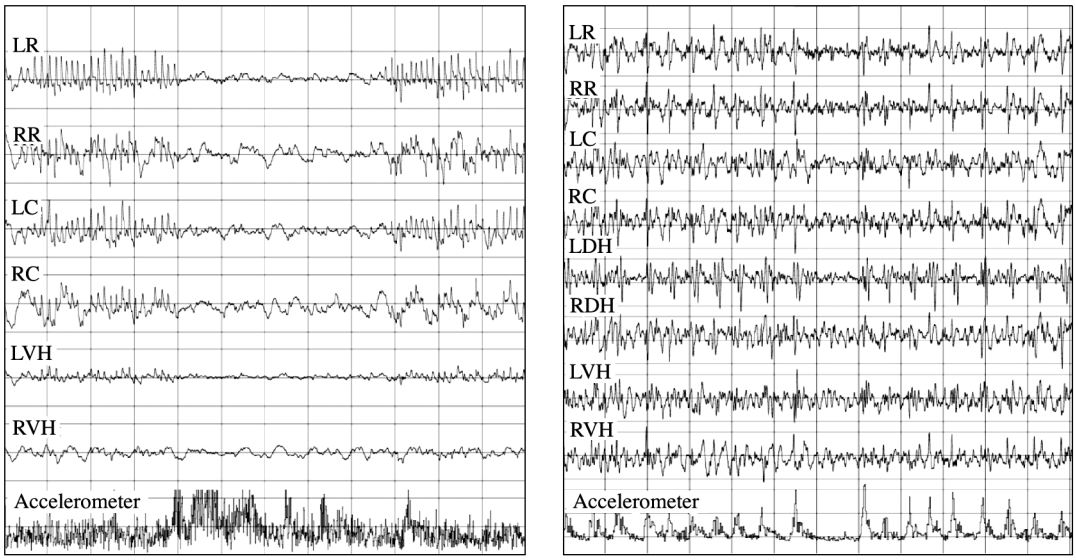

a *b*

Fig. 5. Electrographic seizures in rats six months after TBI. *a*) Nonmotor seizures in the form of behavior arrest. *b*) Motor seizures in the form of myoclonia. LR – Left rostral areas of the cortex; RR – right rostral areas of the cortex; LC – left caudal areas of the cortex; RC – right caudal areas of the cortex; LVH – left ventral hippocampus; RVH – right ventral hippocampus; LDH – left dorsal hippocampus; RDH – right dorsal hippocampus.

ratio of the phases of the sleep–waking cycle or the duration of cycles in rats of the TBI or SO groups. The mean duration of the sleep–waking cycle was 47 ± 5 min. The mean duration of the NREM sleep phase in 12-month-old animals in this study was 26 ± 4 min (49 ± 3%), that of the REM phase was 5 ± 1 min (9 ± 1%), and that of waking was 17 ± 1 min (42%). Sleep structure in six-month-old animals prior to craniotomy reported in [Komoltsev et al., 2017] was: the NREM sleep phase was 38.8 ± 1.0%, that of REM sleep was 9.5 ± 0.4%, and that of the waking phase was 51.4 ± 1.1%. As compared with these results, all rats at age 12 months showed some reduction in the proportion of waking and an increase in the proportion of NREM sleep (with age, the sleep–waking cycle showed changes of about 10% as an increase in the proportion of NREM sleep and a decrease in waking).

Discussion. *Hippocampal sclerosis after TBI*. The type of HS depends on the severity of gliosis and the pattern of neuron death in different hippocampal fields [Malmgren and Thom, 2012; Blümcke et al., 2013]. Type 1 HS in humans is characterized by gliosis and neuron death in fields CA1 and CA4, while type 2 HS occurs mainly in field CA1 and type 3 HS occurs mainly in field CA4 (DG) [Blümcke et al., 2013; Blümcke et al., 2017]. Our data indicate that TBI in rats leads to an increase in the number of glial cells in the long-term period (Nissl staining) with no change in the number of astrocytes. Thus, the increase in the number of glial cells is due to the non-astrocyte glia, probably microglial cells; it is also possible that some proportion is accounted for by lymphoid cells. In rats with TBI, changes in both the number and morphology of astrocytes revealed pronounced asymmetry: the number of astrocytes and the extent of gliosis were greater in the ipsilateral hippocampus (dentate gyrus (DG) and field CA3) than the contralateral. In addition, field CA3 in rats with TBI showed thinning of the pyramidal layer, associated with a decrease in the number of neurons in this area. Thinning of this layer correlated with the number of astrocytes and was greater in rats with marked gliosis. The morphological picture of damage in rats of the TBI group could thus be related to type 3 HS in humans. Animals of the SO group showed only isolated hippocampal gliosis. Changes in the hippocampus (hippocampal sclerosis) were described in rats with posttraumatic epilepsy after lateral hydrodynamic blows – affecting fields CA1 and CA3–CA4 – which corresponded to type 1 hippocampal sclerosis in humans [Aronica et al., 2017]. The type of HS determines the severity of memory impairments in patients with epilepsy – patients with types 1 and 3 HS show pronounced impairments to declarative memory, while type 2 HS produces less marked defects [Coras et al., 2014]. However, the type of hippocampal damage may have relevance both for dementias and other pathologies. Some authors have identified age-related hippocampal sclerosis as a separate nosology [Nelson et al., 2013]. Use of the hippocampal sclerosis classification to assesses the sequelae of TBI has potential for the analysis of all comorbid states associated with trauma. Aberrant neurogenesis and sprouting occurring on the background of neuroinflammation in the dentate gyrus of the hippocampus may be a component of the pathogenesis of PTE [Gulyaeva et al., 2010; Parent and Kron, 2010; Klein et al., 2018]. The changes described above were most pronounced in the dentate gyrus and field CA3. We also observed disper-

sion of the pyramidal layer in hippocampal field CA3. The literature currently contains no correlates for this manifestation. The phenomenon of dispersion of the granular cell layer in patients with epilepsy is seen in the dentate gyrus of the hippocampus and is associated with impairments to neuron migration [Houser, 1990] and impairments to the functioning of reelin [Haas et al., 2002].

The properties of the neuroglia identified in our studies point to its activated state. The glial polarization profile (microglia – M1/M2 and astrocytes – A1/A2) have a complex time dynamic after TBI: in chronic neuroinflammation, as in acute, there is a dominance of proinflammatory polarization of the glia [Biswas and Mantovani, 2012; Jin et al., 2012; Donat et al., 2017]. This is characterized by hyperproduction of proinflammatory mediators (IL-1β, IFN-α and -γ, POC), whose presence in turn leads to continuing neuron death associated with behavioral impairments [Puntambekar et al., 2018]. Secondary brain tissue damage and neuron death include the mechanisms of apoptosis and necrosis [Thompson et al., 2005]. Apoptosis after TBI occurs on the background of inflammatory changes [Dixon et al., 2017] and the extent of apoptosis reaches a maximum in the cortex and hippocampus 1–2 weeks after trauma [Luo et al., 2002].

Anxiety behavior in the long-term period of TBI. Mental disorders are common in patients after TBI: the risk of developing depression in the long-term period in TBI patients reaches 60%, as compared with only 8–10% among the general population [Fann et al., 2009; Scholten et al., 2016]. In elderly people with histories of TBI, the risk of depression is twice as high as that in the general population [Albrecht et al., 2015]. Trauma patients are also at elevated risk of other mental disorders such as anxiety, post-traumatic stress disorder, and suicidal thoughts and behavior [Iverson et al., 2011; Fisher et al., 2016; Zaninotto et al., 2016; Brandel et al., 2017].

In rats, age-related hippocampal gliosis was accompanied by changes in behavior: pronounced decreases in mobility and the appearance of behavioral elements which could be induced by increases in the animals' anxiety (increased duration of time spent in the closed arms with no change in the number of center crossings). Behavioral impairments in traumatized animals were more marked – in comparison with rats of the SO group, elements of exploratory activity in post-trauma rats were quite minor. Experimental studies of rats with TBI have demonstrated cognitive impairments [Thompson et al., 2006 Gurkoff et al., 2013] which could persist for six months [Dixon et al., 1999]. Signs of anxiety were apparent one and three months after TBI but not at six months [Jones et al., 2008]. Our data indicated that at six months, all animals showed reductions in motor activity, which could "mask" behavioral impairments due to TBI and explain the results presented above (our own and published data). It is interesting that modeling of diffuse TBI by acceleration (a model of trauma in which diffuse damage is induced by strong acceleration and arrest of the movement of a fixed experimental animal), which was not accompanied by remote neuroinflammation in the hippocampus, produced no signs of anxiety behavior, changes in locomotor behavior, or marked cognitive impairments at one, three, or 12 months after TBI [Arulsamy et al., 2018, 2019]. Depression-like behavior in the Porsolt test was seen at one and three months after trauma [Arulsamy et al., 2018, 2019]. These data point to the exclusive importance of hippocampal damage for formation of behavioral impairments. Thus, at age one year, along with formation of hippocampal gliosis, animals showed reductions in motor activity and displayed signs which could be induced by elevated anxiety. In rats with TBI, hippocampal gliosis was asymmetric and corresponded to type 3 HS ipsilaterally, and behavioral impairments were more severe (decreased exploratory activity).

Epileptic seizures in the long-term period of TBI. At six months after trauma, epileptic motor (myoclonic) and nonmotor (behavior arrest) seizures were recorded in two of the three animals, which corresponded to previously published data and evidenced the validity of the model used [D'Ambrosio et al., 2004; Pitkänen and Immonen, 2014; Pitkänen et al., 2017]. In addition, we found an increase in discharge duration in the cortex and asymmetry of spikes in the hippocampus. The mechanisms of formation and the role of spike-wave discharges in the cortex in the literature have been actively discussed [Rodgers et al., 2015]. Prolonged discharges in the cortex may be evidence of epileptic seizures in the animals [Dudek and Bertram, 2010]. The small number of animals in this group was due to technical difficulties on recording the EEG in the long-term period: the skull bones were deformed six months after the first operation, resulting in difficulty implanting the electrodes. This study was unable to demonstrate correspondence between electrophysiological and morphological impairments. Our further studies will address this question. However, the presence of epileptic seizures is an important characteristic of the model, evidencing the occurrence of epileptogenic processes in at least some of the rats with TBI with the morphological pattern of damage described above.

Changes in the sleep–waking cycle were identical in rats of the SO and TBI groups – a predominance of NREM sleep over waking was seen, as compared with previously published data from young animals [Komoltsev et al., 2017]. In the early period of TBI, impairments to the sleep–waking cycle consisted of a decrease in the proportion of REM sleep.

Conclusions

1) Six months after craniotomy, rats showed astrocyte gliosis in the hippocampus. In rats with TBI, gliosis was asymmetrical and was accompanied by thinning of hippocampal layer CA3 (which may correspond to human HS type 3) and an increase in the number of nonastrocyte glial cells.

2) Six months after craniotomy, all rats showed pronounced reductions in movement activity. Behavioral el-

ements which could be induced by increases in anxiety occurred on the background of these changes. In rats with TBI, behavioral abnormalities were more severe, mainly due to decreases in elements of exploratory activity.

3) Epileptiform activity was recorded in the cortex six months after TBI, along with asymmetry of spike activity in the hippocampus, and motor (movement arrest) and nonmotor (myoclonic) epileptic seizure were recorded in two rats, evidencing the occurrence of epileptogenic processes in at least some rats with TBI.

This work was supported by the Russian Foundation for Basic Research (Grant Nos. 19-015-00258) (studies of the long-term stage of TBI) and 18-315-00146 (studies of remote hippocampal damage).

REFERENCES

Albrecht, J. S., Kiptanui, Z., Tsang, Y., et al., "Depression among older adults after traumatic brain injury: A national analysis," *Am. J. Clin. Geriatr. Psychiatry*, **23**, No. 6, 607–614 (2015).

Aronica, E., Mühlebner, A., van Vliet, E. A., and Gorter, J. A., "Characterization of pathology," in: *Models of Seizures and Epilepsy*, Academic Press (2017), 2nd ed., pp. 139–160.

Arulsamy, A., Corrigan, F., and Collins-Praino, L. E., "Cognitive and neuropsychiatric impairments vary as a function of injury severity at 12 months post-experimental diffuse traumatic brain injury: Implications for dementia development," *Behav. Brain Res.*, **365**, 66–76 (2019).

Arulsamy, A., Teng, J., Colton, H., et al., "Evaluation of early chronic functional outcomes and their relationship to pre-frontal cortex and hippocampal pathology following moderate-severe traumatic brain injury," *Behav. Brain Res.*, **348**, 127–138 (2018).

Bailey, K. R. and Crawley, J. N., *Anxiety-Related Behaviors in Mice*, CRC Press/Taylor & Francis (2009).

Biswas, S. K. and Mantovani, A., "Orchestration of metabolism by macrophages," *Cell Metab.*, **15**, No. 4, 432–437 (2012).

Blümcke, I., Spreafico, R., Haaker, G., et al., "Histopathological findings in brain tissue obtained during epilepsy surgery," *N. Engl. J. Med.*, **377**, No. 17, 1648–1 (2017).

Blümcke, I., Thom, M., Aronica, E., et al., "International consensus classification of hippocampal sclerosis in temporal lobe epilepsy: A Task Force report from the ILAE Commission on Diagnostic Methods," *Epilepsia*, **54**, No. 7, 1315–1329 (2013).

Brandel, M. G., Hirshman, B. R., McCutcheon, B. A., et al., "The association between psychiatric comorbidities and outcomes for inpatients with traumatic brain injury," *J. Neurotrauma*, **34**, No. 5, 1005–1016 (2017).

Christensen, J., "The epidemiology of posttraumatic epilepsy," *Seminars in Neurology*, **35**, No. 03, 218–222 (2015).

Cole, J. H., Leech, R., and Sharp, D. J., "Prediction of brain age suggests accelerated atrophy after traumatic brain injury," *Ann. Neurol.*, **77**, No. 4, 571–581 (2015).

Coras, R., Pauli, E., Li, J., et al., "Differential influence of hippocampal subfields to memory formation: insights from patients with temporal lobe epilepsy," *Brain*, **137**, No. 7, 1945–1957 (2014).

D'Ambrosio, R., Fairbanks, J. P., Fender, J. S., et al., "Post-traumatic epilepsy following fluid percussion injury in the rat," *Brain*, **127**, No. 2, 304–314 (2004).

Dixon, C. E., Kochanek, P. M., Yan, H. Q., et al., "One-year study of spatial memory performance, brain morphology, and cholinergic markers after moderate controlled cortical impact in rats," *J. Neurotrauma*, **16**, No. 2, 109–122 (1999).

Dixon, K. J., "Pathophysiology of traumatic brain injury," *Phys. Med. Rehab. Clin. North Am.*, **28**, No. 2, 215–225 (2017).

Donat, C. K., Scott, G., Gentleman, S. M., and Sastre, M., "Microglial activation in traumatic brain injury," *Front. Aging Neurosci.*, **9**, 208 (2017).

Dudek, F. E. and Bertram, E. H., "Counterpoint to 'what is an epileptic seizure?' by D'Ambrosio and Miller," *Epilepsy Curr.*, **10**, No. 4, 91–94 (2010).

Fann, J. R., Hart, T., and Schomer, K. G., "Treatment for depression after traumatic brain injury: A systematic review," *J. Neurotrauma*, **26**, No. 12, 2383–2402 (2009).

Fann, J. R., Ribe, A. R., Pedersen, H. S., et al., "Long-term risk of dementia among people with traumatic brain injury in Denmark: a population-based observational cohort study," *Lancet Psychiatry*, **5**, No. 5, 424–431 (2018).

Fisher, L. B., Pedrelli, P., Iverson, G. L., et al., "Prevalence of suicidal behaviour following traumatic brain injury: Longitudinal follow-up data from the NIDRR Traumatic Brain Injury Model Systems," *Brain Inj.*, **30**, No. 11, 1311–1318 (2016).

Gulyaeva, N. V., "Aberrant neurogenesis in adult epileptic brain: compensatory or pathologic," *Neurochem. J.*, **4**, No. 2, 84–89 (2010).

Gurkoff, G. G., Gahan, J. D., Ghiasvand, R. T., et al., "Evaluation of metric, topological, and temporal ordering memory tasks after lateral fluid percussion injury," *J. Neurotrauma*, **30**, No. 4, 292–300 (2013).

Haas, C. A., Dudeck, O., Kirsch, M., et al., "Role for reelin in the development of granule cell dispersion in temporal lobe epilepsy," *J. Neurosci.*, **22**, No. 14, 5797–5802 (2002).

Houser, C. R., "Granule cell dispersion in the dentate gyrus of humans with temporal lobe epilepsy," *Brain Res.*, **535**, No. 2, 195–204 (1990).

Iverson, K. M., Hendricks, A. M., Kimerling, R., et al., "Psychiatric diagnoses and neurobehavioral symptom severity among OEF/OIF VA patients with deployment-related traumatic brain injury: a gender comparison," *Womens Health Issues*, **21**, No. 4, S210–S217 (2011).

Jin, X., Ishii, H., Bai, Z., et al., "Temporal changes in cell marker expression and cellular infiltration in a controlled cortical impact model in adult male C57BL/6 Mice," Nataf S. (ed), *PLoS One*, **7**, No. 7, e41892, (2012).

Jones, N. C., Cardamone, L., Williams, J. P., et al., "Experimental traumatic brain injury induces a pervasive hyperanxious phenotype in rats," *J. Neurotrauma*, **25**, No. 11, 1367–1374 (2008).

Jorge, R. and David, A., "Mood disorders after TBI," *Psychiatr. Clin. North Am.*, **76**, 211–220 (2012).

Kabadi, S. V., Hilton, G. D., Stoica, B., et al., "Fluid-percussion-induced traumatic brain injury model in rats," *Nat. Protoc.*, **5**, No. 9, 1552–1563 (2010).

Klein, P., Dingledine, R., Aronica, E., et al., "Commonalities in epileptogenic processes from different acute brain insults: Do they translate?" *Epilepsia*, **59**, No. 1, 37–66 (2018).

Komoltsev, I. G., Frankevich, S. O., Shirobokova, N. I., et al., "The early electrophysiological sequelae of dosed traumatic brain injury in rats," *Zh. Nevrol. Psikhiat.*, **118**, No. 10, 21–26 (2018).

Komoltsev, I. G., Frankevich, S. O., Shirobokova, N. I., et al., "The acute period in modeling of traumatic brain injury in rats: immediate convulsions, damage to the functional areas of the neocortex, and degradation of behavior," *Zh. Nevrol. Psikhiat.*, **119**, No. 11, 90–93 (2019).

Komoltsev, I. G., Levshina, I. P., Novikova, M. R., et al., "The acute posttraumatic period in rats is accompanied by an anxiety state and reduction in the proportion of REM sleep," *Zh. Vyssh. Nerv. Deyat.*, **67**, No. 2, 1–15 (2017).

Luo, C., Jiang, J., Lu, Y., and Zhu, C., "Spatial and temporal profile of apoptosis following lateral fluid percussion brain injury," *Chin. J. Traumatol.*, **5**, No. 1, 24–27 (2002).

Malmgren, K. and Thom, M., "Hippocampal sclerosis Origins and imaging," *Epilepsia*, **53**, supplement 4, 19–33 (2012).

McIntosh, T. K., Vink, R., Noble, L., et al., "Traumatic brain injury in the rat: Characterization of a lateral fluid-percussion model," *Neuroscience*, **28**, No. 1, 233–244 (1989).

Nelson, P. T., Smith, C. D., Abner, E. L., et al., "Hippocampal sclerosis of aging, a prevalent and high-morbidity brain disease," *Acta Neuropathol.*, **126**, No. 2, 161–177 (2013).

Parent, J. M. and Kron, M. M., "Neurogenesis and epilepsy," in: *Jasper's Basic Mechanisms of the Epilepsies* [Internet], National Center for Biotechnology Information (US), Bethesda (MD) (2012), 4th ed.

Pitkänen, A. and Immonen, R., "Epilepsy related to traumatic brain injury," *Neurotherapeutics*, **11**, No. 2, 286–296 (2014).

Pitkänen, A., Kyyriäinen, J., Andrade, P., et al., "Epilepsy after traumatic brain injury," in: *Models of Seizures and Epilepsy*, Elsevier (2017), pp. 661–681.

Puntambekar, S. S., Saber, M., Lamb, B. T., and Kokiko-Cochran, O. N., "Cellular players that shape evolving pathology and neurodegeneration following traumatic brain injury," *Brain Behav. Immun.*, **71**, 9–17 (2018).

Rodgers, K. M., Dudek, F. E., and Barth, D. S., "Progressive, seizure-like, spike-wave discharges are common in both injured and uninjured Sprague–Dawley rats: Implications for the fluid percussion injury model of post-traumatic epilepsy," *J. Neurosci.*, **35**, No. 24) (2015).

Scholten, A. C., Haagsma, J. A., Cnossen, M. C., et al., "Prevalence of and risk factors for anxiety and depressive disorders after traumatic brain injury: A systematic review," *J. Neurotrauma*, **33**, No. 22, 1969–1994 (2016).

Simon, D. W., McGeachy, M. J., Bayır, H., et al., "The far-reaching scope of neuroinflammation after traumatic brain injury," *Nat. Rev. Neurol.*, **13**, No. 3, 171–191 (2017).

Thompson, H. J., LeBold, D. G., Marklund, N., et al., "Cognitive evaluation of traumatically brain-injured rats using serial testing in the Morris water maze," *Restor. Neurol. Neurosci.*, **24**, No. 2, 109–114 (2006).

Thompson, H. J., Lifshitz, J., Marklund, N., et al., "Lateral fluid percussion brain injury: a 15-year review and evaluationm," *J. Neurotrauma*, **22**, No. 1, 42–75 (2005).

Vezzani, A., Auvin, S., Ravizza, T., and Aronica, E., "Glia-neuronal interactions in ictogenesis and epileptogenesis: role of inflammatory mediators," *Jasper's Basic Mechanisms of the Epilepsies* [Internet], National Center for Biotechnology Information (US), Bethesda (MD) (2012), 4th ed.

Wood, R. L., "Accelerated cognitive aging following severe traumatic brain injury: A review," *Brain Inj.*, **31**, No. 10, 1270–1278 (2017).

Zaninotto, A. L., Vicentini, J. E., Fregni, F., et al., "Updates and current perspectives of psychiatric assessments after traumatic brain injury: A systematic review," *Front. Psychiatry*, **7**, 1–14 (2016).